Microstructural study and magnetic properties of SmCo-type 2:17 magnets

E. Estevez Rams[+], *J. Fidler*[‡], *A. Penton Madrigal*[+], *R.Lora Serrano*[+"]
+ Laboratorio de Analisis Estructural. IMRE-Facultad de Fisica. Universidad de la Habana. San Lazaro y L. CP 10400. C. Habana. Cuba
‡ Institute for Applied and Technical Physics. Technical University of Vienna. Wiedner Haupstr. 8-10, Vienna, Austria.
"On leave from Facultad de Ciencias. Departamento de Fisica. Universidad de Oriente
Corresponding author: Ernesto Estevez Rams - Facultad de Fisica. Universidad de la Habana
San Lazaro y L. CP 10400 - C. Habana. Cuba - Email: estevez@lae.ff.oc.uh.cu
Fax: (+537) 33-4247 - Phone: (+537) 70-7666

Abstract

Samples of Sm2Co17-type magnets with different coercivity and quenching rate were studied by transmission electron microscopy. Microstructure of Sm_2Co_{17}-type magnets is described. The high coercivity samples showed a well developed cellular microstructure with thick $Sm(Co,Cu)_5$ walls. The hexagonal platelet phase runs as long straight lines crossing the cell walls. The low coercivity sample showed a chaotic precipitation of the $Sm(Co,Cu)_5$ phase while the hexagonal platelet phase are more densely packed and runs as short straight lines in the TEM micrographs. Quantitative measurement of platelet density and cell size were made and correlated with the coercive field value.

1 - Introduccion

Sm_2Co_{17} type magnets still hold the best magnetic properties at elevated temperature due to the low Curie temperature of $Nd_2Fe_{14}B$ magnets and the low spontaneous magnetization of the SmCo5 magnet [1]. In spite of the extensive literature in Sm_2Co_{17} magnets, renewed interest has emerged due to its applications in electric vehicles and in the defense sector [1]. In all this cases, the high temperature magnetic behavior of this magnet is the main area of focus.

The high temperature magnetic behavior of Sm_2Co_{17} is still not well understood. Tellez et. al [2] has proposed a nucleation driven mechanism for the coercivity mechanism at elevated temperatures in commercial $Sm_2(Co,Fe,Cu,Zr)_{17}$ magnets, while J.F.Liu et. al observed a easy domain wall movement at low applied fields followed by pinning at higher fields [3]. Also there has been in the recent literature some controversy over the exact role of the hexagonal platelet phase, also known as Z-phase, in the coercivity of the Sm_2Co_{17} magnet. While it has been generally assumed that the platelet phase acts primarily as diffusion paths modifying the phase ordering in the magnet [4], it has been argued that the intersection of the Z-phase with the 1:5 cell wall could act as pinning sites [5] with a decisive contribution to coercivity. On the other hand Skomski, following micromagnetic calculations, has argued that the Z-phase does not contribute significantly to the pinning mechanism responsible for the measured high coercivity value [6].

In this paper we present an electron microscopy study of two type of samples of $Sm_2(Co,Fe,Cu,Zr)_{17}$ magnet. The samples underwent the same heat treatment but were cooled at two different quenching rates resulting in different coercivity values. First the experimental procedure will be described, followed with a short description of the microstructure observed in Sm_2Co_{17}-type magnets. Finally the microstructure of both types of samples will be studied and its implication on the observed magnetic properties will be discussed.

2 - Materials and Methods

Two samples of commercial $Sm_2(Co,Fe,Cu,Zr)_{17}$ were studied, both underwent sintering at 1180° C and solutionizing treatment at 1150° C but with different quenching rates. As a result of the different cooling rate, the slowly quenched samples showed a rather low coercivity, while the rapidly quenched samples exhibit a large coercive field value. Table I summarizes the magnetic properties of the analyzed samples.

All samples were ground, polished and finally thinned in a ion mill at 5kV to obtain electron transparency. The

samples were observed in a JEOL 200 CX analytical transmission electron microscope (TEM) equipped with an energy dispersive microanalysis system.

3 - Results and discussion

Microstructure of Sm_2Co_{17}-type magnets.

Due to its comparatively low magnetocrystalline anisotropy (K1 ~ 3100 kA/m), pure Sm_2Co_{17} magnets does not develop a high coercivity value [2]. In order to obtain the required coercive field value needed to achieve high density energy products, a composition containing Fe, Cu and Zr besides Sm and Co is used usually with a composition around $Sm(Co_{0.66}Fe_{0.25}Cu_{0.05}Zr_{0.02})_{7.7}$. While Fe is mainly added to increase spontaneous magnetization, its amount is limited by the fact that Sm_2Fe_{17} exhibits an easy plane anisotropy [1]. Cu and Zr, on the other hand, are essential for developing, after a lengthy heat treatment, a complex microstructure responsible of the high coercivity values in a pinning driven magnet.

The main phases in the Sm_2Co_{17}-type magnets is the Sm_2Co_{17} rhombohedral phase (SG: R3m, a=8.395 nm c=12.216 nm, structure type: Th_2Zn_{17}). The low solubility of Cu in the Sm_2Co_{17}-R matrix phase induces the precipitation of $SmCo_5$ (hexagonal, SG: P6/mmm, a=5.002 nm c=3.964 nm, structure type: $CaCu_5$) enriched in Cu. Zr is believed to favor the occurrence of stacking faults in the basal plane of the Sm_2Co_{17}-R phase, resulting in the formation of a unit cell high, hexagonal Sm_2Co_{17} platelet phase (hexagonal, SG: Pb3/mmc, a=8.360 nm c=8.515 nm, structure type: Th_2Ni_{17}) which is also known as Z-phase [5].

It is believed that the Zr enriched platelet phase acts as diffusion path for Cu, this results in the coherent precipitation of the $Sm(Co,Cu)_5$ phase forming a maze of ideally rhombohedral cells as Figure 1a shows. Figure 1b is a scheme of an ideal rhombohedral cell showing the different phases and its crystallographic relation.

The perfect individual cells when observed by TEM with the c-axis in the plane of the sample, shows a characteristic rhombic geometry (Figure 2a). The same cells when observed in a plane perpendicular to the c-axis, can exhibit two geometry depending on the sectional cut of the rhombohedral cell. If the section corresponds to a plane near the apex of the cell, a triangular geometry will result (Figure 2b), otherwise an hexagonal geometry will be observed (Figure 2c).

As already mentioned the occurrence of stacking faults in the basal plane of the Sm_2Co_{17}-R phase results in, a unit cell height, Sm_2Co_{17}-H platelet phase. The difference between the Sm_2Co_{17} rhombohedral and hexagonal structure is a different stacking sequence of the same structural layer unit [7]. Stacking fault results in a local hexagonal sequence. Planar faulting can occur with and without twining. Figure 3a and b shows the occurrence of both type of faulting. Twinning can readily be seen as a change of contrast across the platelet phase. The platelet Z-phase can be seen running through the $Sm(Co,Cu)_5$ cell wall phase (figure 3b). Figure 4 shows the [1211] zone axis, electron diffraction pattern with extra spots due to described twinning, figure 4b is an enlarged view of the same diffraction pattern showing the indexed reflections corresponding to the Sm_2Co_{17}-R matrix and the extra twin spots.

$SmCo_5$ structure is also closely related to the Sm_2Co_{17} phases. $SmCo_5$ results from the substitution of a pair of so called Co-dumbbells by a Sm atom in the Sm_2Co_{17} phases [8]. $Sm(Co,Cu)_5$ precipitates oriented with respect to the Sm_2Co_{17}-R phase such that it minimize the strain between both phases, the orientation relationship was found by electron diffraction to be

$$(0001)_{2:17} \parallel (0001)_{1:5} \qquad [1100]_{2:17} \parallel [1120]_{1:5}$$

in agreement with previous studies [8].

Microstructure of different quenched samples

Real Sm_2Co_{17}-type magnets do not exhibit a perfect cell structure. Frequent disruption of cell wall and other imperfections are also observed which are usually related with the magnetic properties of the sample.

Rapidly quenched sample exhibits high coercivity values and correspondingly, the microstructure of figure 5a shows a well-defined cell structure with a rather thick cell wall and a long platelet phase running through the micrograph. When seen in a plane perpendicular to the c-axis (figure 5b) the microstructure of the same sample exhibits a maze of cells. The accommodation of stress results also in the bending of the cell walls and the deformation of the rhombohedral cell structure. This is particularly evident when the microstructure is seen perpendicular to the c-axis. Cell size measured along and perpendicular to the c-axis gave a average value of 260 nm and 112 nm, respectively. The optical micrograph of figure 6 shows that precipitation occurs homogeneously over all the sample.

The slowly quenched samples show a different microstructure (figure 7). The precipitation of the $Sm(Co,Cu)_5$ occurs chaotically without forming any defined geometrical structure as seen in figure 7a. The Z-phase is seen more densely packed forming short segments. Cell size was measured in regions with a slightly more defined structure in the S3 sample, the measurement along and perpendicular to the c-axis gave a average value of 174 nm and 76 nm, respectively. S4 showed such disrupted microstructure that cells could not be defined yet measured. When observed in a plane perpendicular to the c-axis (figure 7b), the cellular structure again is smaller and size and less well defined.

Platelet density was measured in both types of samples. For the S1 and S2 sample an average value of 45 mm^{-1} was obtained, while for the S3 and S4 samples and average value of 63 mm^{-1} was measured.

In figure 8 the behavior of jHc vs. platelet density is shown together with a section for both good coercive field samples and bad coercive field samples, the micrographs clearly shows that platelet density in S3 is higher than in S1. Platelets phase in the bad coercivity sample (S3), exhibit shorter segments than in the S1 sample. The measurement confirms that as the platelet density increases a decrease of coercivity is found.

In the slowly quenched sample a higher density of platelet phase is found. Platelets are forming short segments which can be seen frequently intersecting $Sm(Co,Cu)_5$ precipitates in the Sm_2Co_{17}-R matrix. In spite of the occurrence of both Z-phase and the described intersection the pinning mechanism in this samples proved to be insufficient to attain high coercive field values.

Although there is a relation between the platelet density and the coercivity in our samples it is by no means an easy task to separate the contribution of the platelet phase, on one hand, to the development of the cell structure and on the other, to the magnetic behavior. If the occurrence of a higher density of faulting leads to a chaotic precipitation of $Sm(Co,Cu)_5$ phase without formation of cell structure, high coercivity values are not attained. Our microstructural studies tend to suggest that is the cell structure who plays a relevant role in the pinning mechanism of the Sm_2Co_{17}-type magnet. In order to understand the magnetic role of the platelet Z-phase more reliable measurements of the magnetic parameters of such phase are needed. From the microstructural point of view, TEM studies of the exact nature of the intersection of the platelet phase and the $Sm(Co,Cu)_5$ phase has to be made.

Acknowledgment

E. Estevez Rams which to acknowledge the financial support of the OAD.

Samples	S1	S2	S3	S4
$(BH)_{max}$ [kJ/m³]	214	214	206	182
JH_c [kA/m]	>1600	>1600	750	420
Js [T]	1.09	1.10	1.11	1.12

Table1: Magnetic properties of the samples after heat treatment.

References

1. See, K. J. Strnat, in Ferromagnetic Materials, edited by E. P. Wohlfarth and K. H. J. Buschow (North-Holland, New York, 1988), Vol. 4, p. 134.

1. S. Liu, E. P. Hoffman, J.R. Brown, IEEE Trans. Magn. **33** (1997), p. 3859.

2. J. C. Tellez-Blanco, X. C. Kou, R. Grossinger, E. Estevez-Rams, J. Fidler, B. M. Ma, J. Appl. Phys., **82** (8) 1997, p. 3928.

3. J. F.Liu, Y. Zhang, G. C. Hadjipanayis, J. Magn. Magn. Mater. **202** (1999) p. 69.

4. J. Fidler, J.Magn. Magn. Mater. **30** (1982), p.58.

5. M. Katter, J. Weber, W. Assmus, P. Schrey, W. Rodewald, IEEE Trans. Magn. **32** (1996) p. 4815.

6. R. Skomski, J. Appl. Phys., **81** (1997), p. 5627.

7.E. Estevez Rams, PhD. Dissertation thesis , 1996.

8. K. H.Morimoto, M. Watanabe and T. Takeshita, IEEE Trans. Magn. **MAG-23** (1987), p.2708.

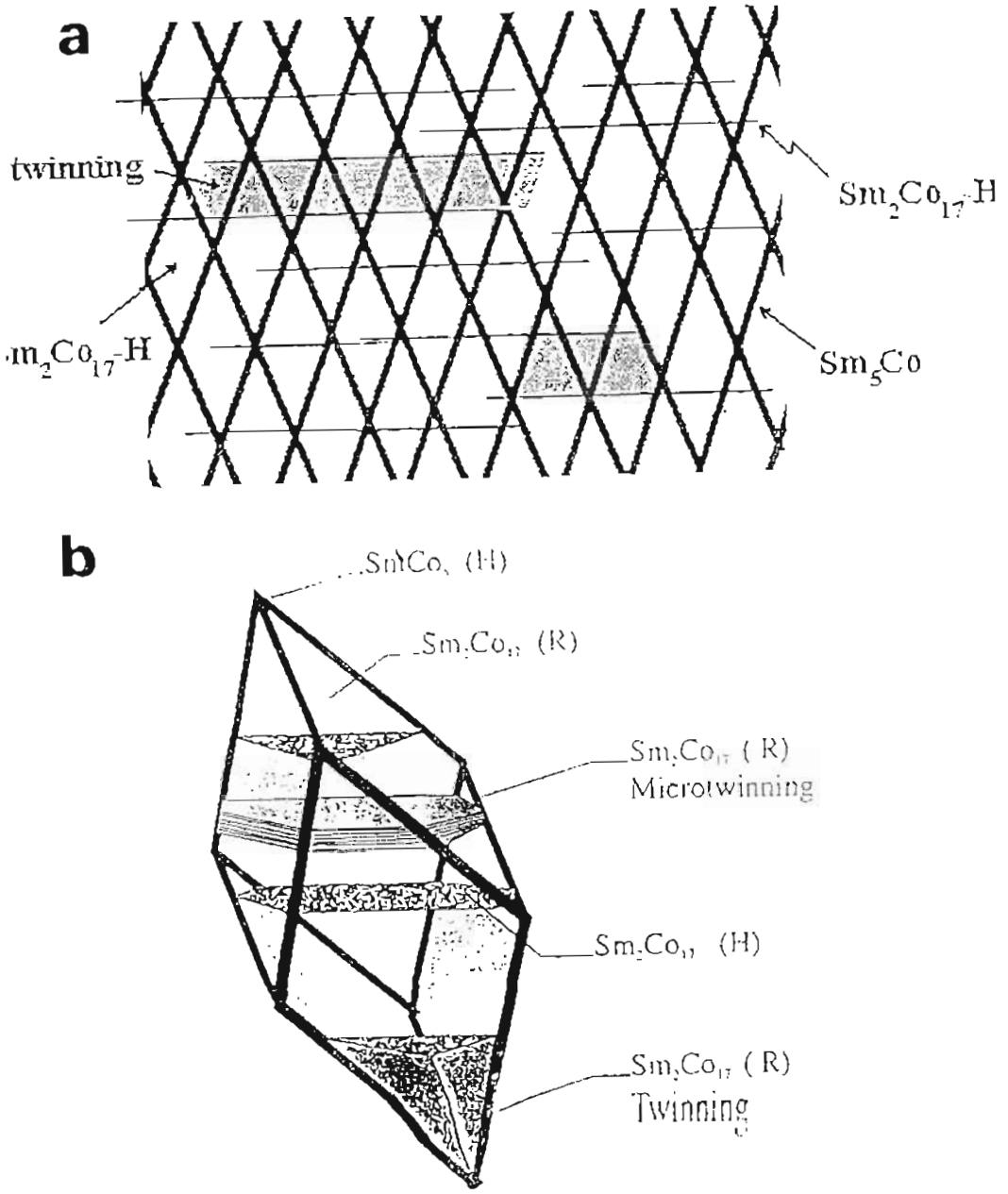

Figure 1. (a) 2D model of the ideal microstructure of the Sm_2Co_{17}-type magnet (b) Ideal rhombohedral cell.

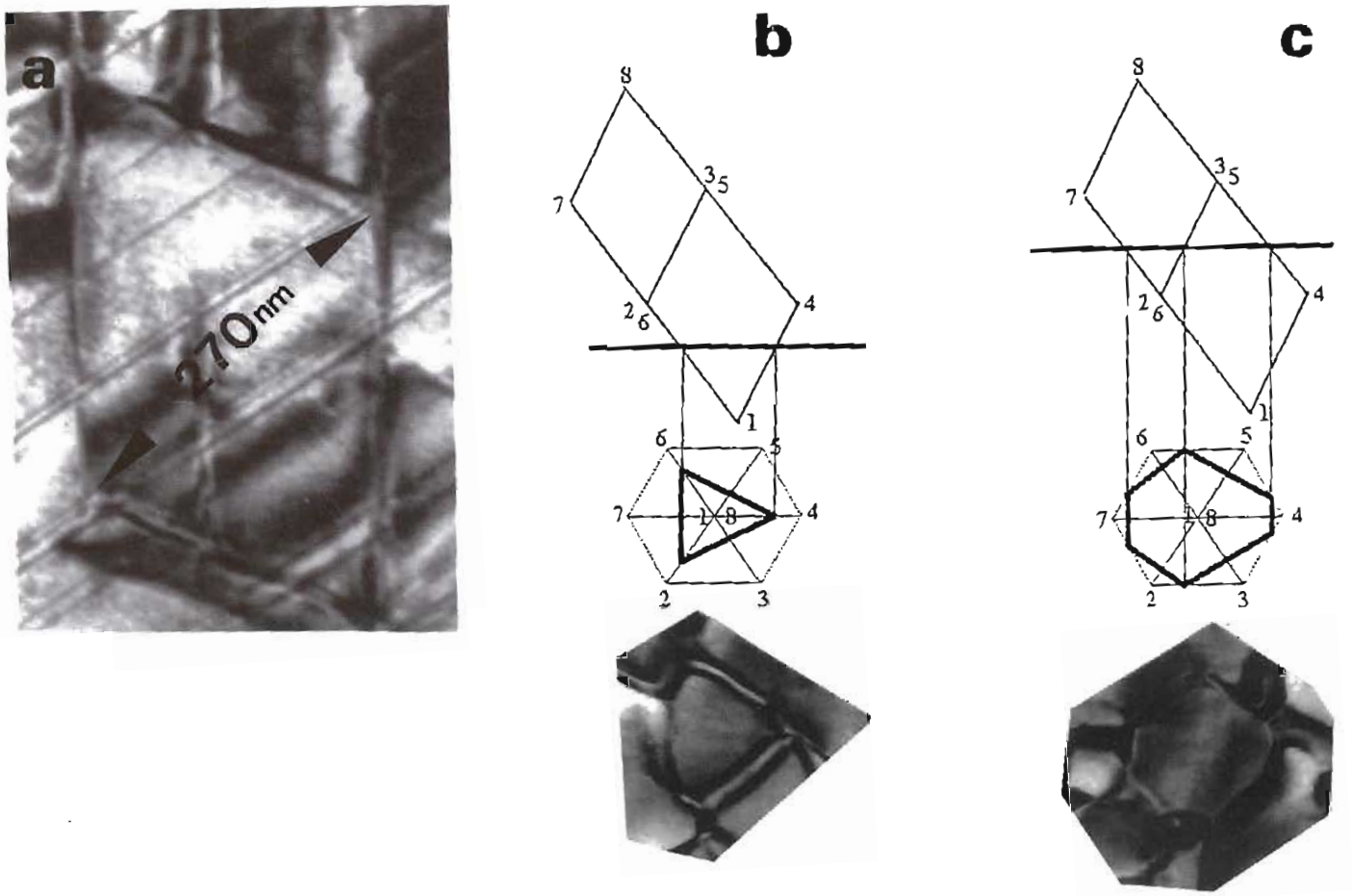

Figure 2. Projection of the rhombohedral cell when observed in TEM under different directions and sectional cuts. (a) c-axis in the plane of the micrograph. (b) c-axis perpendicular to the plane of the micrograph, sectional cut near the apex of the rhombohedral cell. (c) sectional cut through the middle of the rhombohedral cell.

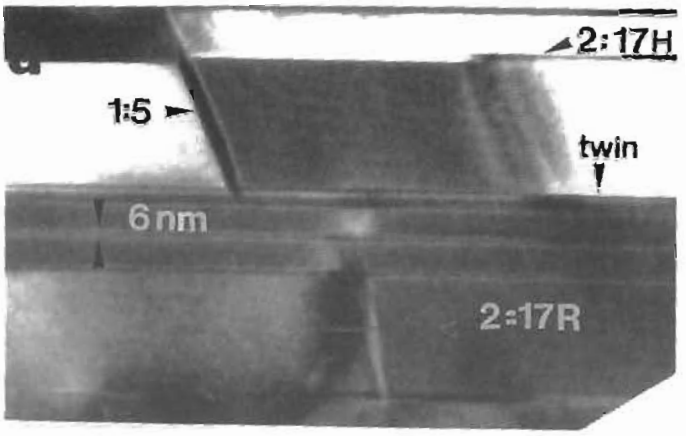

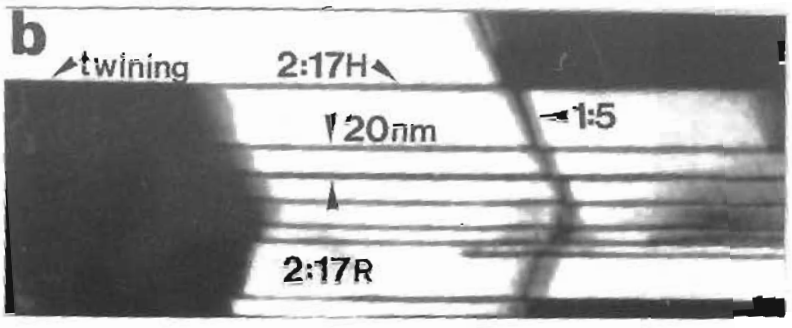

Figure 3. Planar faulting and twinning in the basal plane of the Sm_2Co_{17}-R matrix. Stacking faults are seen as straight lines forming the hexagonal platelet phase Sm_2Co_{17}-H (Z-phase). When stacking faults are accompanied by twinning it can be seen as a change of contrast through the platelet phase. In (b) the hexagonal Z-phase can be seen running across the $Sm(Co,Cu)_5$ cell wall.

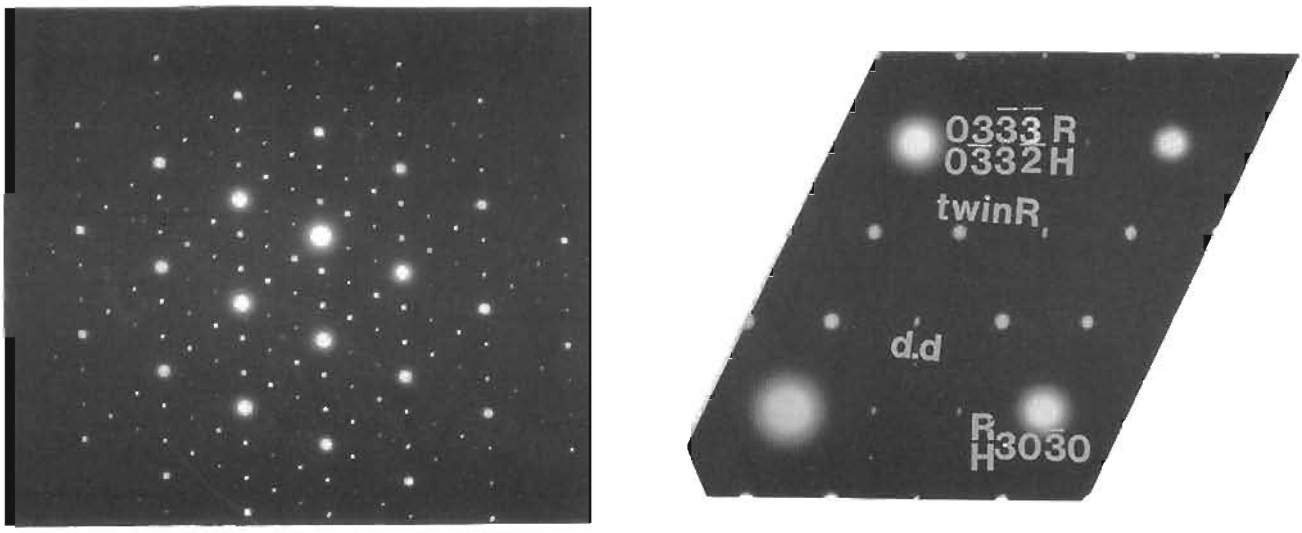

Figure 4. Electron diffraction pattern [1211] Zone axis with extra spots due to twinning and double diffraction. (b) Enlarged view of the diffraction pattern. d.d corresponds to double diffraction reflections while twinR corresponds to twinning extra reflections. R and H are rhombohedral and hexagonal reflection, respectively.

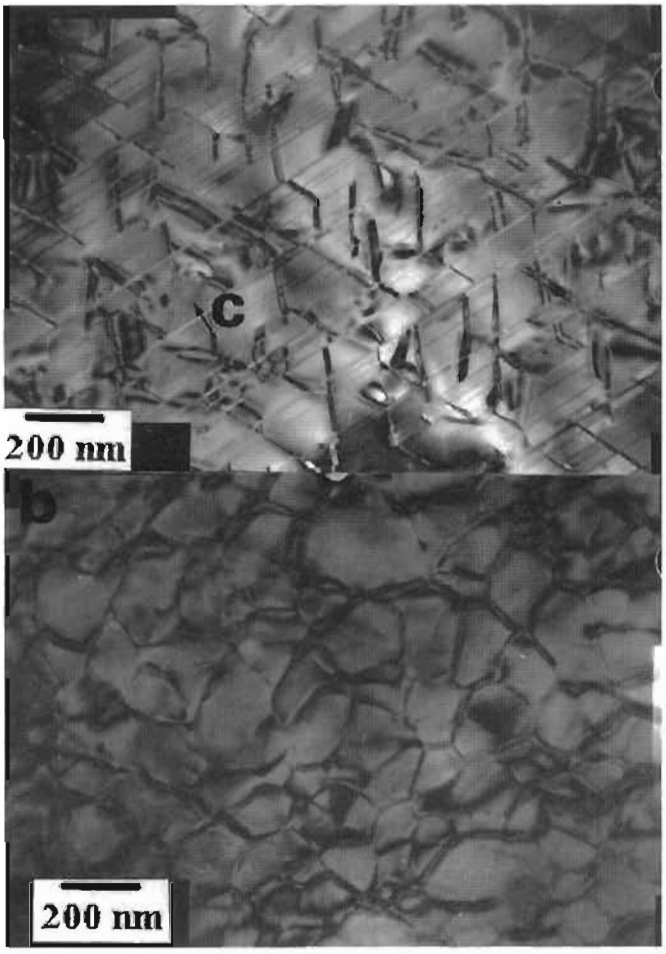

Figure 5. Microstructure of high coercivity S1sample (a) Thick $Sm(Co.Cu)_5$ cell walls are seen with the platelet phase as long straight lines crossing the cell walls. The microstructure has a well-defined cell structure. (b) Sample seen perpendicular to the c-axis. Maze of cells can be seen with average size of 112 nm. S2 showed similar microstructure.

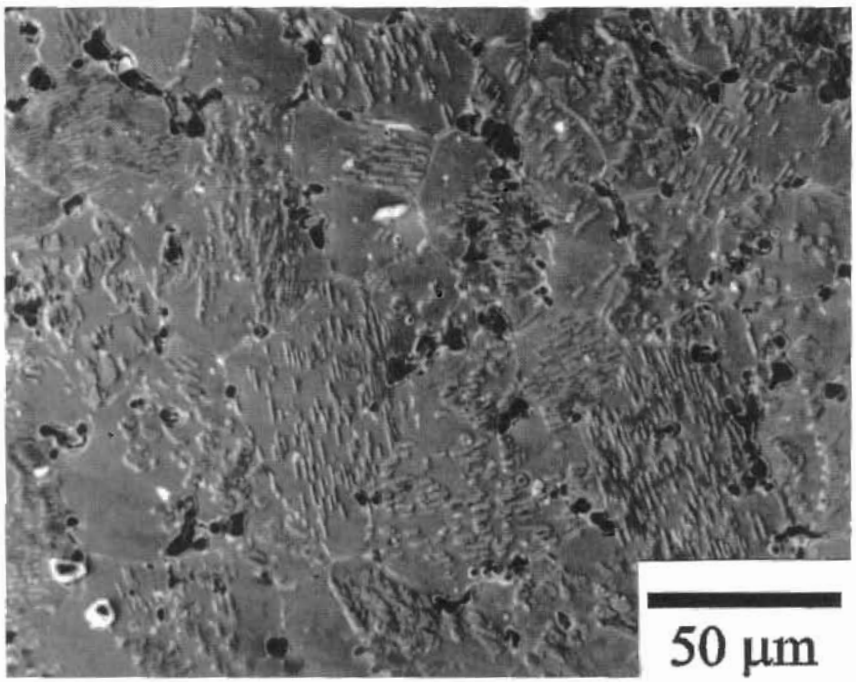

Figure 6. Optical micrograph of high coercivity S1 sample. Precipitation inside the Sm_2Co_{17}-R grains can be seen. Precipitation occurs throughout the sample. S2 showed a similar behavior.

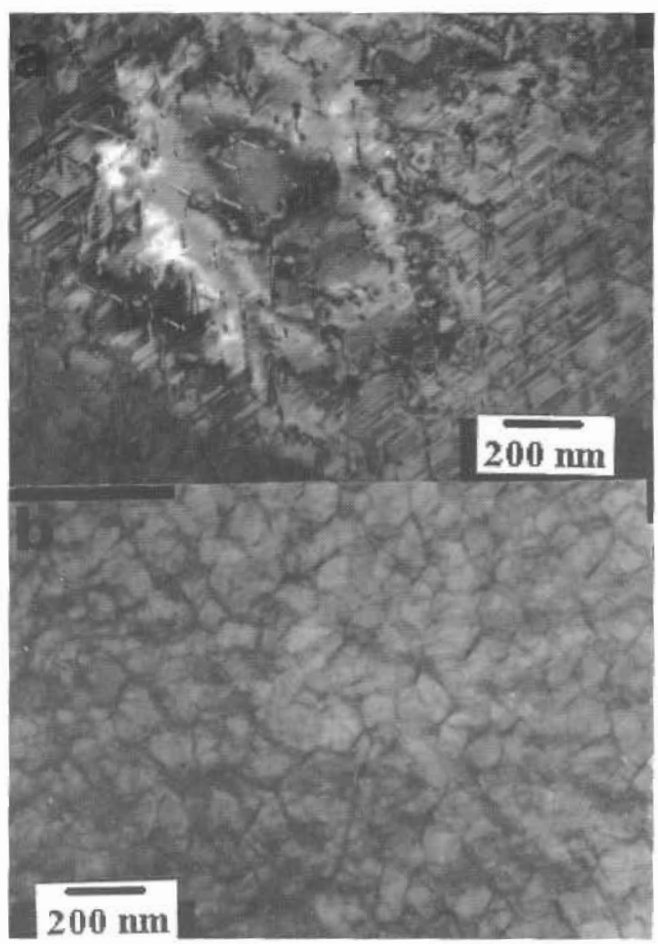

Figure 7. Microstructure of low coercivity S3 sample. (a) Random precipitation of the $Sm(Co,Cu)_5$ phase can be seen. No c ·llular structure can be defined. Z-phase runs as short platelets densely distributed over the micrograph. (b) When seen in a plane perpendicular to the c-axis, the cell structure is smaller in size and less well defined than in the high coercivity samples.

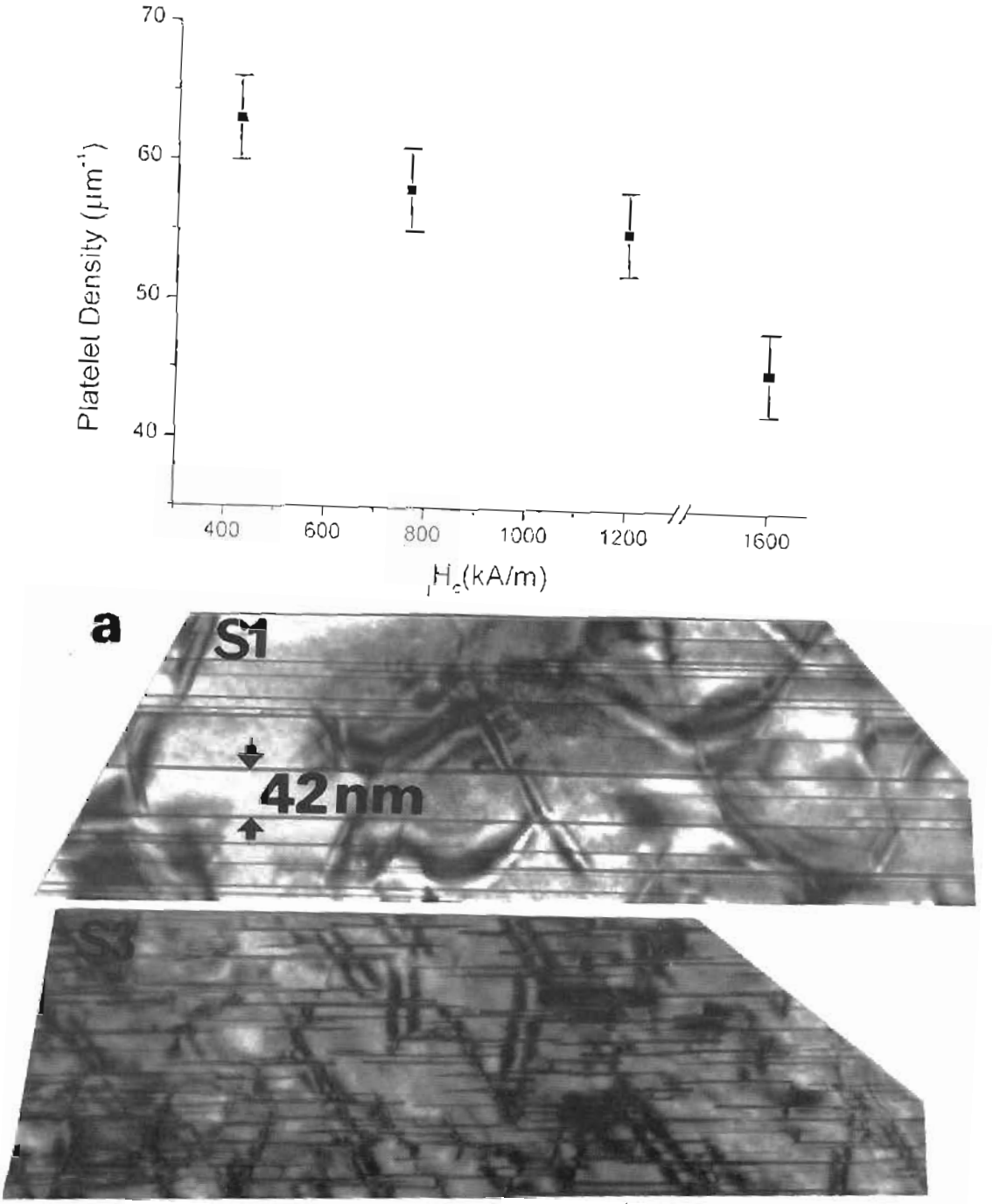

Figure 8. $_iH_c$ versus platelet density. (a) High coercivity sample S1 showing long straight lines corresponding to the hexagonal platelet phase, in the low coercivity sample S3 the platelet phase is seen as shorter segments more densely packed.